Developing a Robust Acquisition System for Fringe Projection Profilometry

IOP Conf. Series: Journal of Physics: Conf. Series **1247** (2019) 012053 doi:10.1088/1742-6596/1247/1/012053

Developing a Robust Acquisition System for Fringe Projection Profilometry

Jesus Pineda,[1] **Andres G. Marrugo,**[1] **and Lenny A. Romero**[2]

[1]Facultad de Ingenieria, Universidad Tecnologica de Bolivar, Cartagena, Colombia
[2]Facultad de Ciencias Basicas, Universidad Tecnologica de Bolivar, Cartagena, Colombia

E-mail: jesuspinedacastro@outlook.com

Abstract. Since Fringe Projection Profilometry (FPP) is an intensity-based coding strategy, it is prone to improper optical setup arrangement, surface texture and reflectance, uneven illumination distribution, among others. These conditions introduce errors in phase retrieval which lead to an inaccurate 3-D reconstruction. In this paper, we describe a dynamic approach toward a robust FPP acquisition in challenging scenes and objects. Our aim is to acquire the best possible fringe pattern image by adjusting the object closer to an ideal system-object setup. We describe the software implementation of our method and the interface design using LabVIEW. Experimental results demonstrate that the proposed method greatly reduces sources of error in 3-D reconstruction.

1. Introduction

Fringe Projection Profilometry (FPP) is a widely used technique based on structured illumination for optical three-dimensional (3D) shape measurement. It provides a 3D topography of objects in a non-contact manner, with high resolution, and fast data processing. However, since FPP is an intensity-based coding strategy, it is prone to improper optical setup arrangement, surface texture and reflectance, uneven illumination distribution, among other problems.

In recent years, we have seen a tendency toward robust FPP acquisition systems in challenging scenes and objects. For instance, Sheng et al. [1] proposed a dynamic projection theory for FPP to avoid overexposed areas in the object. The method identifies the overexposed pixels, it maps them back to the projector and modifies the projection pattern to reduce the number of overexposed points. Alternatively, Peng et al. [2, 3] proposed an adaptive projection method which relies on fringe patterns with spatial pitch variation to achieve improved accuracy and coverage for an object being measured. However, modifying the projection pattern is not always possible, especially in setups with high-resolution analog projectors. Many authors have also proposed temporal coding schemes [4, 5] in which many patterns are projected on to the surface of the object to achieve robustness. However, they are time-consuming and require the acquisition of many images, which is not suitable for a dynamic scene.

In this paper, we present an acquisition interface for robust FPP acquisition. In the same fashion as over- and under-exposed region detection in images is important in machine vision

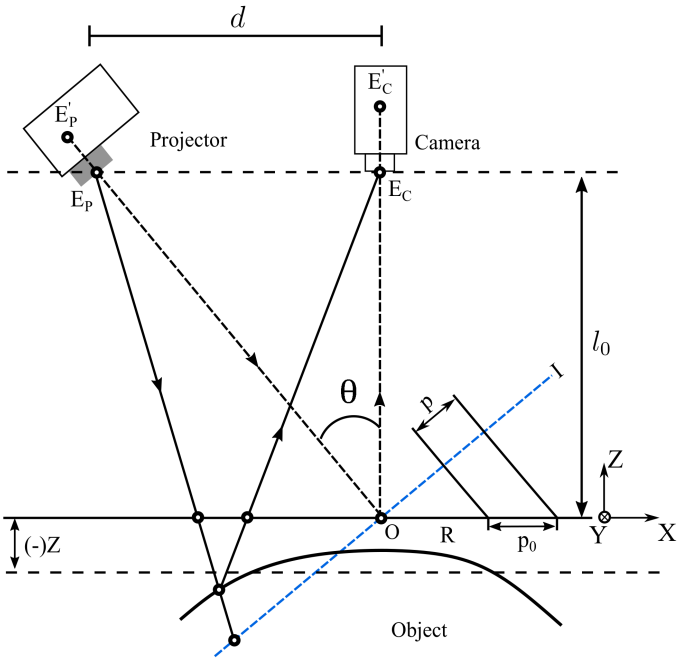

Figure 1: Fringe projection system.

and photography, our approach provides a much-needed feedback in FPP systems for quality evaluation of fringe patterns during acquisition.

2. Method

In a typical FPP set-up, a fringe projector, and a camera are positioned in a triangulation-based arrangement as depicted in Fig. 1. The optical axis $E'_p - E_p$ of the projector lens crosses the optical axis $E'_c - E_c$ of the camera lens at a point O on a plane R, which serves as a reference to measure the height of the object $z(x,y)$. d is the distance between the projector and the camera, and l_0 is the distance between the camera and the plane R. The fringe pattern image (with period p) is formed by the projector lens on plane I through the point O. By projecting the fringe pattern onto the object, the deformed pattern observed through the camera can be modeled as [6]

$$I(x,y) = \alpha \left\{ r(x,y) \left[a_0(x,y) + b(x,y) \cos\left(\Phi(x,y)\right) \right] + a_1(x,y) \right\} \ , \tag{1}$$

where $a_0(x,y)$ represents the projection lighting and $b(x,y)$ is the contrast of the fringe pattern. $\Phi(x,y) = 2\pi f_0 x + \phi(x,y)$, where $\phi(x,y)$ is the phase modulations resulting from the object height distribution and $f_0 = \cos(\theta)/p$ is the carrier frequency. $a_1(x,y)$ is the ambient light entering directly to the camera. $r(x,y)$ and α denotes the reflectivity of the object surface and the camera sensitivity, respectively. From Eq. (1), the average intensity $I'(x,y)$ and the intensity modulation $I''(x,y)$ are given by

$$I'(x,y) = \alpha r(x,y) a_0(x,y) + \alpha a_1(x,y) \ , \tag{2}$$

$$I''(x,y) = \alpha r(x,y) b(x,y) \ . \tag{3}$$

Likewise, the data modulation $\lambda(x,y)$ is expressed as

$$\lambda(x,y) = \frac{r(x,y)b(x,y)}{r(x,y)a_0(x,y) + a_1(x,y)} \quad . \tag{4}$$

To achieve a high-quality coding, $\lambda(x,y)$ must be close to 1. According to Eq. (4), FPP is prone to surface texture and reflectance [1], uneven illumination distribution[7, 8], fringe contrast, and so on. There are other unwanted effects that may induce phase recovery errors in FPP. For instance, the viewing angle results in the obscuration of part of the surface by an elevated feature [9, 10]. Or surfaces with local defects that produce local shear in the fringes [11]. The aforementioned conditions affect the recovered wrapped phase leading to an inaccurate 3-D reconstruction. In the next section, we implemented an acquisition interface for robust FPP recovery, so as to improve the quality of 3-D measurements.

3. Toward a Robust Acquisition

In this section, we present a robust acquisition interface for FPP systems based on two approaches for quality evaluation of fringe patterns. The first approach consists of an intensity profile along the middle cross-section of the fringe pattern image for monitoring the contrast of the fringes $b(x,y)$, as well as its interaction with the reflectivity of the surface $r(x,y)$, and the ambient light $a_1(x,y)$. The second approach is a phase residue-based quality metric which we proposed in Ref. [12] to identify error-prone areas during acquisition. Our purpose is to give users graphical feedback to obtain the best possible fringe pattern image by adjusting the object closer to an ideal system-object setup. Therefore, assuring a more homogeneous illumination, more uniform fringe contrast and an accurate 3D measurement. In Fig. 2 we show the acquisition interface in LabVIEW.

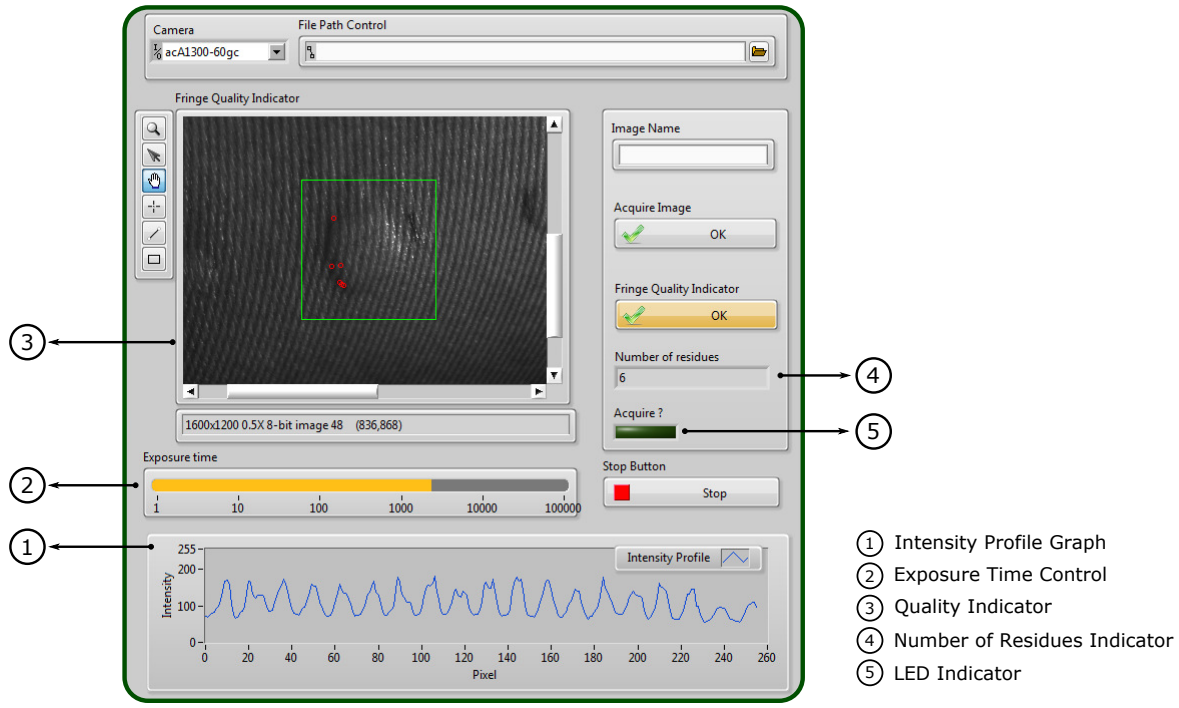

Figure 2: Acquisition interface in LabVIEW.

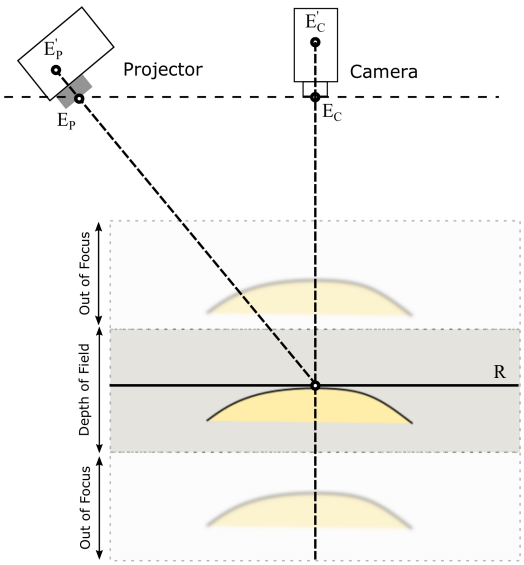

Figure 3: Contrast Adjustment process.

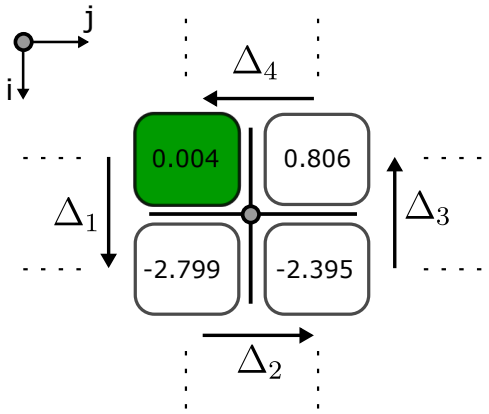

Figure 4: Residue calculation example.

3.1. Intensity Modulation Adjustment

As shown in Fig. 2, we use a `Waveform Graph` to display the intensity profile. We set the intensity-axis limits to be between 0 and 255 for an ideal fringe pattern. The main idea is to use the feedback provided by the intensity graph to obtain a large intensity modulation, $I''(x,y)$, by adjusting the position of the object relative to the 3-D reconstruction system, as well as modifying acquisition parameters such as the exposure time. For instance, if the surface reflectivity is small, according to Eq. 3, the camera sensitivity, α, must be large for assuring an optimal intensity modulation. This condition is compensated by increasing the camera exposure time or aperture. Our acquisition interface relies on a `Numeric Control` to modify the exposure time attribute value using a `Property Node`. From Eq. (4), the ambient light also plays an important role in the intensity modulation adjustment process. To achieve a high fringe contrast, the ambient lighting conditions must be negligible.

A higher fringe contrast is also possible by modifying the position of the object relative to the 3-D reconstruction system. As is illustrated in Fig. 3, as the object is positioned closer to the reference plane R, the contrast is maximized. This must be kept within a certain depth of field. If the object is out of focus, the contrast of the fringes will decrease.

3.2. Error-Prone Areas Detection

During acquisition, a phase residue analysis is computed to identify the error-prone areas from each fringe image to avoid complex phase retrieval algorithms [13]. This method relies on Fourier Transform Profilometry (FTP) [14, 15] for phase retrieval due to its single-shot nature. The residue calculation can be understood by examining the array in Fig. 4, which contains samples of a wrapped phase function $\Phi(x,y)$. The phase derivatives are computed discretely as local two-point phase differences. However, the estimate of the true gradient is obtained by wrapping the differences of wrapped phase as in the following expression [11],

$$\sum_{k=1}^{4} \Delta_k = \mathbb{W}\left\{\phi(i+1,j) - \phi(i,j)\right\} + \mathbb{W}\left\{\phi(i+1,j+1) - \phi(i+1,j)\right\} \\ + \mathbb{W}\left\{\phi(i,j+1) - \phi(i+1,j+1)\right\} + \mathbb{W}\left\{\phi(i,j) - \phi(i,j+1)\right\} \quad , \tag{5}$$

where (i, j) is the pixel index and $\mathbb{W}(.)$ is the wrapping operator that wraps the phase differences into the interval $(-\pi, \pi]$ as $\Delta_k = \mathrm{mod}(\Delta\phi + \pi, 2\pi) - \pi$. A residue is found when Eq. 5 is different from zero. For example, referring to Fig. 4 to detect if the green pixel is a residue we obtain $\Delta_1 = -2.803$, $\Delta_2 = 0.404$, $\Delta_3 = -3.082$, $\Delta_4 = -0.802$, which yield $\sum_{k=1}^{4} \Delta_k = -6.283$. In effect, this pixel is a residue and indicates an area of poor quality.

To provide graphical feedback, the locations of residues are plotted on top of the grabbed image using the `Quality Indicator` in Fig. 2. The acquisition condition is met if the amount of residues is lower or equal than a predefined threshold (ideally zero residues). The number of residues is shown using a `Numeric Indicator` and a `LED indicator` displays the acquisition condition. If the `LED indicator` is `ON`, the acquisition condition is met. Otherwise, the LED will stay `OFF`.

4. Experiments and Results

The experimental setup consists of two parts: a projection system and an observation system (see Fig. 1). The projection system was an LED pattern projector (Optoengineering LTPRHP3W-W) that contains a stripe pattern of 200 lines with a line thickness of 0.02 mm with a projection lens of 8-mm focal length. The observation system was a CMOS camera (Basler acA1600-60gm 1602x1202 pixels) with an objective lens of 16-mm focal length.

The object under inspection is the forearm of a test subject which exhibits an inflammation on the surface of the skin. Our interest focus on obtaining the 3-D information of the inflammation or papule. In Fig. 5(A) the `Quality Indicator` is displayed highlighting phase residues near the edges of the deformation. These phase residues impede the accurate measurement of the 3D data as shown in Fig. 5(B). In error phase areas, a sophisticated phase unwrapping algorithm must be employed to estimate the optimal phase values such as minimum L^p-norm algorithms, Quality-guided algorithms, among others [11]. In Fig. 5(C) the subject was asked to slowly change the pose until the number of residues decreased. According to the `Quality Indicator`, by slightly modifying the pose of the object, the phase residues disappear. We assume the object to be non-deformable during the adjustment. The recovered 3D shape is shown in Fig. 5(D).

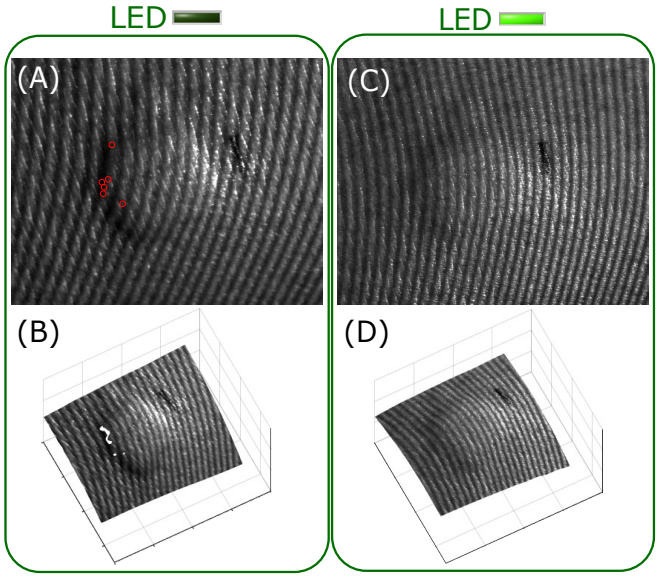

Figure 5: A: Initial fringe image with residues displayed and B: recovered 3D shape. C: Optimized fringe image with zero residues displayed and D: recovered 3D shape.

5. Conclusions

We have developed a robust acquisition interface for FPP systems which relies on a residue-based quality metric and a contrast intensity monitoring for quality evaluation of fringe pattern during acquisition. Our experiments showed that problems associated with erroneous phase retrieval could be avoided during acquisition by having information related to error-prone areas their locations. Additionally, our method enables the acquisition under more favorable 3D shape recovery conditions with an online residue analysis.

Acknowledgment

This work has been partly funded by Colciencias (Fondo Nacional de Financiamiento para la Ciencia, la Tecnología y la Innovación Francisco José de Caldas) project 538871552485, and by Universidad Tecnológica de Bolívar projects C2018P005 and C2018P018. Authors thank Dirección de Investigaciones, Universidad Tecnológica de Bolívar for the support. J. Pineda thanks Universidad Tecnológica de Bolívar for a Masters degree scholarship.

References

[1] Sheng, H., Xu, J., and Zhang, S. (2017). Dynamic projection theory for fringe projection profilometry. *Applied Optics*, **56(30)**, 8452-8460.
[2] Peng, T., and Gupta, S. K. (2007). Model and algorithms for point cloud construction using digital projection patterns. *Journal of Computing and Information Science in Engineering*, **7(4)**, 372-381.
[3] Peng, T., and Gupta, S. K. (2008). Algorithms for generating adaptive projection patterns for 3D shape measurement. *Journal of Computing and Information Science in Engineering*, **8(3)**, 031009.
[4] Zhang, C., Xu, J., Xi, N., Zhao, J., and Shi, Q. (2014). A robust surface coding method for optically challenging objects using structured light. *IEEE Transactions on Automation Science and Engineering*, **11(3)**, 775-788.
[5] Li, S., Da, F., and Rao, L. (2017). Adaptive fringe projection technique for high-dynamic range three-dimensional shape measurement using binary search. *Optical Engineering*, **56(9)**, 094111.
[6] Zhang, S., and Yau, S. T. (2009). High dynamic range scanning technique. *Optical Engineering*, **48(3)**, 033604.
[7] Vargas, R., Pineda, J., Marrugo, A. G., and Romero, L. A. (2016). Background intensity removal in structured light three-dimensional reconstruction. In *Signal Processing, Images and Artificial Vision (STSIVA), 2016 XXI Symposium on* (pp. 1-6). IEEE.
[8] Luo, F., Chen, W., and Su, X. (2016). Eliminating zero spectra in Fourier transform profilometry by application of Hilbert transform. *Optics Communications*, **365**, 76-85.
[9] Bone, D. J. (1991). Fourier fringe analysis: the two-dimensional phase unwrapping problem. *Applied Optics*, **30(25)**, 3627-3632.
[10] Stavroulakis, P., Sims-Waterhouse, D., Piano, S., and Leach, R. (2017). Flexible decoupled camera and projector fringe projection system using inertial sensors. *Optical Engineering*, **56(10)**, 104106.
[11] Pritt, M. D., and Ghiglia, D. C. (1998). *Two-dimensional phase unwrapping: theory, algorithms, and software*. Wiley.
[12] Pineda, J., Vargas, R., Romero, L. A., Meneses, J., and Marrugo, A. G. (2018). Fringe Quality Map for Fringe Projection Profilometry in LabVIEW. *Opt Pura Apl*, **51(4)**, 50302:1-8.
[13] Wang, X., Fang, S., Zhu, X., and Li, Y. (2018), Phase unwrapping of interferometric fringes based on a mutual information quality map and phase recovery strategy, *Optical Engineering*, **57(11)**, 1–16.
[14] Takeda, M., and Mutoh, K. (1983). Fourier transform profilometry for the automatic measurement of 3-D object shapes. *Applied Optics*, **22(24)**, 3977-3982.
[15] Marrugo, A. G, Pineda, J., Romero, L. A., Vargas, R., and Meneses, J. (2018). *Fourier Transform Profilometry in LabVIEW*, Digital Systems, Asadpour Vahid (Ed.), Publisher: IntechOpen, DOI: dx.doi.org/10.5772/intechopen.78548